

## Order-disorder phase transition in random-walk networks

Fernando J. Ballesteros

*Observatorio Astronómico, Universidad de Valencia, Edificio Institutos de Investigación, Pol. La Coma, Paterna 46980, Valencia, Spain*

Bartolo Luque

*Departamento de Matemática Aplicada y Estadística, ETSI Aeronáuticos, Universidad Politécnica de Madrid, Plaza Cardenal Cisneros 3, Madrid 28040, Spain*

(Received 16 July 2004; revised manuscript received 15 October 2004; published 14 March 2005)

In this paper we study in detail the behavior of random-walk networks (RWN's). These networks are a generalization of the well-known random Boolean networks (RBN's), a classical approach to the study of the genome. RWN's are also discrete networks, but their response is defined by small variations in the state of each gene, thus being a more realistic representation of the genome and a natural bridge between discrete and continuous models. RWN's show a clear transition between order and disorder. Here we explicitly deduce the formula of the critical line for the annealed model and compute numerically the transition points for quenched and annealed models. We show that RBN's and the annealed model of RWN's act as an upper and a lower limit for the quenched model of RWN's. Finally we calculate the limit of the annealed model for the continuous case.

DOI: 10.1103/PhysRevE.71.031104

PACS number(s): 05.40.Fb, 02.50.-r, 02.70.Uu

### I. INTRODUCTION

Biological networks [1] are typically made up of a large number of units interacting with each other in a highly nonlinear way, often exhibiting complex dynamics. Neural systems, where the units are neurons with chemolectrical interactions, or the genome, where the units are genes with protein interactions, are typical examples of biological networks.

A classical approach to gene networks involves discrete dynamical systems based on random Boolean functions. Such Boolean networks are formed by a set of  $N$  genes or automata (labeled  $i=1, 2, \dots, N$ ) where each gene has two possible states  $x_i \in \{0, 1\}$ , where 0 stands for inactive (non-protein production) and 1 for active (protein production). Each gene  $i$  is connected with  $K$  other genes  $\{i_1, i_2, \dots, i_K\}$ . We generate in this way a network whose dynamics is described by a set of  $N$  equations  $\{x_i^{t+1} = f_i(x_{i_1}^t, x_{i_2}^t, \dots, x_{i_K}^t)\}_{i=1, 2, \dots, N}$ , where  $t$  indicates time and the  $\{f_i\}_{i=1, 2, \dots, N}$  are Boolean functions of  $K$  inputs. The output values and the input automata  $\{i_1, i_2, \dots, i_K\}$  for these functions are typically assigned in a quenched random way. These rules fully describe the so-called random Boolean networks (RBN's) [2] which are among the best known models of biological networks. Extensive analysis has shown that two phases (ordered and disordered) can be defined for RBN's. The existence of an ordered phase in this random systems has been used as support for the idea of "order for free." Also, the presence of a critical point is particularly relevant to complex systems, due to their maximum information transfer properties and high homeostatic stability of attractors. It has been conjectured (edge of the chaos hypothesis) that the boundary separating the ordered and disordered phases will allow the genome to display stability and homeostasis as emergent phenomena arising from criticality [3].

Although RBN's are simple models, they capture the essence of real genetic networks in some cases. An example is

the virus Phage  $\lambda$  model [4], which consists in a coupled pair of cross-inhibitory differential equations. Although continuous in essence, the result in this model of interaction between continuous quantities leads to a basically binary (RBN-like) outcome. Nevertheless, not all models can be approached in the same way. In general, the more complex the network is, the more possible states can be observed, displaying a range of intermediate nonbinary values. The protein concentration produced by gene transcription determines the activation or inhibition of other genes. But it is known that the range of protein concentration produced by genes spans up to two orders of magnitude. Very few genes are strictly on-off switched [5]; rather they show a continuous behavior [6], changing smoothly (without jumps) among different states. In order to handle this continuous behavior, models of many-gene activity based on differential equations have been developed. However, they pose evident computational and analytical problems, because  $N$  genes imply  $N$  coupled, nonlinear differential equations. In [7] a continuous-discrete hybrid set of piecewise linear differential equations is proposed in order to avoid this problem. Unfortunately, it is difficult to obtain analytical results in such continuous or semicontinuous models. A discrete dynamical system would be more manageable.

But how can such diversity of states be included in a discrete system? A desirable feature for a discrete model describing genetic networks will be a set of functions  $\{f_i\}_{i=1, \dots, N}$  such that changes in  $x_i^t$  will take place smoothly, through single and ordered steps among a high number of possible states. The model should also take into account other realistic features, like the fact that the response of genes to stimulation and inhibition by other genes shows saturation in their response. Such is the case for random walk networks (RWN's), proposed in a previous paper [8] as a more realistic representation of the genome. These networks satisfy in a simple way the previous requirements, working with small variations in the gene states, thus being a discrete approach

to differential equations and allowing a comparison with continuous models.

RWN's allow for an analytical treatment and show complex dynamical behavior and order-disorder transitions similar to RBN's [9]—random threshold networks [10] or asymmetric neural networks [11], for example. In fact RBN's are a simple subcase of RWN's.

In Sec. II we present the RWN model more formally, explicitly deducing the critical line for the annealed model in Sec. III. In Sec. IV we show new simulations and compute the transition points for quenched and annealed models. In Sec. V we obtain the stationary automaton-state distribution and show that it is bimodal in the ordered phase. We discuss the differences between the distributions in the annealed and quenched models and show that they are the key to understand the different behavior of both models. Finally we see that RBN's and the annealed model of RWN's are an upper and a lower limit for the quenched model of RWN's, and we calculate the limit for the continuous case of the annealed model.

## II. RWN MODEL DESCRIPTION

RWN's are formed by  $N$  automata  $i \in \{1, 2, \dots, N\}$ , each of them connected with  $K$  other automata  $\{i_1, i_2, \dots, i_K\}$ . Each automaton can be in one of  $s$  possible states ranging from 1 to  $s$ : that is,  $x_i \in \{1, 2, \dots, s\}$ . The changes among states  $x_i^t$  at time  $t$  occur in discrete steps  $\{+1, -1\}$ , defined by an associated function (rule table)  $\phi_i$  of  $K$  variables. Each one of these functions takes as input the values of the  $K$  input automata:  $x_{i_1}, x_{i_2}, \dots, x_{i_K}$ . In contrast to RBN's, in RWN's the output of the associated function does not directly define the new value of the automaton, but just a variation  $+1$  or  $-1$  in its value  $x_i$  and, hence, their link with differential equations. These variations modify the state of a given automaton producing (in the disordered case) a random-walk-like behavior of its value, which gives name to these networks. The dynamics of each automaton is constrained by two reflecting states: 1 and  $s$ . These extreme states represent null activity and saturation activity, respectively, and act as barriers for the automaton. Note that connections and rule tables are randomly generated at the network definition stage but are maintained (quenched) afterwards.

More formally, the evolution of the system is updated synchronously by the iteration of a global mapping  $\mathbf{F}_K: \{1, 2, \dots, s\}^N \mapsto \{1, 2, \dots, s\}^N$  where  $\mathbf{F}_K = (f_1, f_2, \dots, f_N)$ , each  $f_i$  being a function of  $K+1$  arguments:  $K$  automaton values acting as input of automaton  $i$ , plus its own value—i.e.,  $f_i: \{1, 2, \dots, s\}^{K+1} \mapsto \{1, 2, \dots, s\}$  defined by

$$x_i^{t+1} = f_i(x_i^t, \phi_i^t) = \begin{cases} x_i^t + 1 & \text{if } \phi_i^t = +1 \wedge x_i^t \neq s, \\ s & \text{if } \phi_i^t = +1 \wedge x_i^t = s, \\ x_i^t - 1 & \text{if } \phi_i^t = -1 \wedge x_i^t \neq 1, \\ 1 & \text{if } \phi_i^t = -1 \wedge x_i^t = 1, \end{cases} \quad (1)$$

$\phi_i$  being the rule tables:

$$\phi_i: \{1, 2, \dots, s\}^K \mapsto \{+1, -1\}, \quad (2)$$

$$\phi_i = \phi_i(x_{i_1}^t, x_{i_2}^t, \dots, x_{i_K}^t). \quad (3)$$

For example, let us take  $K=2$  and  $s=4$  and the automaton  $i$  with state at time  $t$ ,  $x_i^t=2$ . Let us suppose that its two input automata have states  $x_{i_1}^t=1$  and  $x_{i_2}^t=3$  at time  $t$ . We look for the input combination  $(1, 3)$  in the rule table  $\phi_i$  corresponding to the automaton  $i$  and find the output  $\phi_i(1, 3) = +1$ . Then the value  $x_i^t=2$  is updated to  $x_i^{t+1} = 2 + 1 = 3$  at time  $t+1$ . In the case  $x_i^t=4$  (saturation state) the update would be  $x_i^{t+1}=4$ . Similarly, if the automaton has a value of  $x_i^t=1$  (null activity) and the output is  $\phi_i(1, 3) = -1$ , the update would be  $x_i^{t+1}=1$ .

The rule tables  $\{\phi_i\}_{i=1, \dots, N}$  are randomly generated for a particular system and then maintained (quenched model). As in RBN's, here we can define a new parameter  $p$ , the bias [9], the probability for the output value of  $\phi_i$  to be  $+1$  [and  $-1$  with probability  $(1-p)$ ] when we generate the functions  $\phi_i$  at the beginning [during the network definition stage].

For RWN's with a given number of states  $s$ , two well-defined phases can be found, which are separated by a critical line in the  $p-K$  space.

(i) An ordered phase when the value of the bias  $p$  is far away from 0.5 and/or the connectivity  $K$  is low, in which case the networks freeze in a pattern after a short transient. In this phase almost all of the automata remain in a frozen state.

(ii) A disordered phase otherwise ( $p$  close to 0.5 and/or large values of  $K$ ), where all patterns are lost and the automata appear to be in complete disorder, switching from one state to another apparently at random.

We can observe that for  $s=2$  the state of each automaton  $i$  at time  $t+1$  is independent of its state at  $t$ , depending only on the value of  $\phi_i$ . Thus  $x_i^{t+1} = f_i(x_i^t; \phi_i^t) = f_i(\phi_i^t)$  and an output  $\phi_i^t = +1$  forces  $x_i^{t+1} = 2$  and, similarly, an output  $\phi_i^t = -1$  forces  $x_i^{t+1} = 1$ . Therefore, RWN's reduce to RBN's when  $s=2$ . In this sense, RWN's represent a generalization of RBN's, but with a richer set of available behaviors.

In Fig. 1 we can see a particular example of a RWN in the critical line, with  $N=100$  automata,  $K=2$ ,  $p=0.79$ , and  $s=10$ , which illustrates this complex behavior. In the upper part of the figure we show the level of activity for each automaton as different gray tones and its evolution with time (towards right). The graph in the lower part shows, as an example, the evolution of the activity state of three of the automata, marked with little dots in the vertical axis in the upper graph. It can be seen how, after a transient, the system reaches a complex periodic state.

## III. RWN ANNEALED MODEL

The annealed model, proposed by Derrida and Pomeau [12], consists of studying a simplified model of a system in which its time correlations are destroyed at each time step by randomly redefining the relationships among components of the system and their response functions. In the case of RBN's where it was applied, it consisted in redefining at each time step the  $K$  inputs and the Boolean functions of all the automata. The unmodified model with time correlations is called in this context the quenched model, as the relationship among components and their response functions do not change during its evolution. In RBN's and other systems the

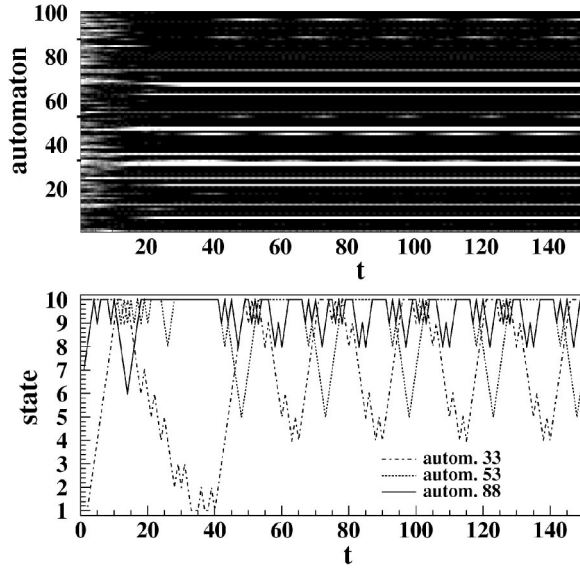


FIG. 1. Example of complex RWN behavior. Top: dynamics of a RWN with  $N=100$  automata,  $K=2$ ,  $p=0.79$ , and  $s=10$ . The horizontal axis represents time steps and the vertical axis shows the 100 automata. Different gray intensities correspond to different states for each automaton, ranging from 1 (white) to 10 (black). Bottom: evolution of the automata states (automata values) in time for the same RWN. For simplicity, only automaton Nos. 33, 53, and 88 are shown (figure from [9]).

boundary between ordered and disordered phases obtained through the annealed model for  $N$  tending to infinity coincides with the boundary of the quenched model, hence the power of this method.

Therefore, following Derrida and Pomeau, we will derive the boundaries separating order and disorder for the RWN annealed model. In order to avoid time correlations, each time step we redefine both the automaton inputs  $i_1, i_2, \dots, i_K$  and functions  $\phi_i$  for each automaton  $i=1, 2, \dots, N$ . The avoiding of time correlations is strictly true for RBN's, but for annealed RWN's the memory dependence is not totally avoided, as  $x_i^t$  influences  $x_i^{t+1}$  [see Eq. (1)]. Nevertheless, the RWN annealed model shows also an ordered-disordered transition and we can compute it as a mean field of the RWN quenched model.

If every time step each automaton  $i$  has  $K$  new inputs and new  $p$ -biased functions  $\phi_i$ , then the state  $x_i$  of each automaton  $i$  behaves as a biased random walk, with probability  $p$  of moving upwards and  $(1-p)$  downwards. The behavior of the automaton  $i$  is constrained by the reflecting states 1 and  $s$ . For this arbitrary automaton  $i$ , we define  $P_n$  as the probability of being in state  $n \in \{1, 2, \dots, s\}$ . If we assume no correlations between automata, we can write the evolution of the probabilities as

$$\begin{cases} P_1(t+1) = (1-p)[P_1(t) + P_2(t)], \\ \vdots \\ P_n(t+1) = (1-p)P_{n+1}(t) + pP_{n-1}(t), \\ \vdots \\ P_s(t+1) = p[P_{s-1}(t) + P_s(t)] \end{cases} \quad (4)$$

with  $n=2, 3, \dots, s-1$ .

Let us take two annealed replicas (with initial state conditions randomly chosen) of the same system that are at time  $t$ :  $C_1(t) \equiv (x_1^{(1)}(t), \dots, x_N^{(1)}(t))$  and  $C_2(t) \equiv (x_1^{(2)}(t), \dots, x_N^{(2)}(t))$ . The overlap in time  $t$ ,  $a(t) \in [0, 1]$ , is defined as the normalized number  $Na(t)$  of elements with common states in  $C_1(t)$  and  $C_2(t)$ . We can interpret  $C_2$  as a perturbation over  $C_1$ . Thus,  $a(t)$  will act as an order parameter when  $t$  tends to infinity. If the system is in the ordered phase,  $a$  will tend to 1 and the initial perturbation will be absorbed. Otherwise, if the system is in the disordered phase,  $a$  will tend to a stable value different from 1 and the perturbation will persist.

Now we need to compute the overlap in  $t+1$  between these two annealed replicas. There will be five cases contributing to its value.

(i) Two equivalent automata  $x_i^{(1)}(t)$  and  $x_i^{(2)}(t)$  are equal [with probability  $a(t)$ ] and also their  $K$  inputs [with probability  $a(t)^K$ ]. The contribution is then  $a^{K+1}(t)$ .

(ii) Two equivalent automata are equal with different input values, but the probability for their input functions  $\phi_i$  to be the same by chance is  $p^2 + (1-p)^2$ . The contribution is then  $a(t)[1 - a^K(t)][p^2 + (1-p)^2]$ .

(iii) Two equivalent automata with different values but the same inputs. In the next time step they can coincide only when their values are  $(s-1, s)$  or  $(s, s-1)$  and  $\phi_i = +1$  or when they are  $(1, 2)$  or  $(2, 1)$  and  $\phi_i = -1$ . The contribution is then

$$(1 - a(t))a^K(t) \frac{2(pP_{s-1}P_s + (1-p)P_1P_2)}{1 - \sum_{n=1}^s P_n^2} \underbrace{\hspace{10em}}_{\Phi(p,s;t)}$$

(iv) Two equivalent automata with different values and different inputs, separated by one unit as in case (iii), but [as in case (ii)] the response of  $\phi_i$  is the correct one by chance. The contribution of this case is, therefore,

$$(1 - a(t))(1 - a^K(t)) \frac{2(p^2P_{s-1}P_s + (1-p)^2P_1P_2)}{1 - \sum_{n=1}^s P_n^2} \underbrace{\hspace{10em}}_{\Omega(p,s;t)}$$

(v) And two equivalent automata with different values and different inputs, separated by two units, the  $\phi$  value for the smaller of them being by chance  $+1$  and  $-1$  for the bigger one. This case contributes with

$$(1 - a(t))(1 - a^K(t)) \frac{2p(1-p) \sum_{n=2}^{s-1} P_{n-1}P_{n+1}}{1 - \sum_{n=1}^s P_n^2} \underbrace{\hspace{10em}}_{\Psi(p,s;t)}$$

Notice that in (iii), (iv), and (v) we have used the conditioned probability as we already know that at  $t$  the two automata have different values. Notice also that the temporal dependence of the distributions  $\{P_n(t)\}_{n=1, \dots, s}$  [as given in Eq. (4)] has been omitted but included in the functions  $\Phi(p, s; t)$ ,  $\Omega(p, s; t)$ , and  $\Psi(p, s; t)$ . Summing all the contributions we obtain the time evolution of the overlap in the annealed model:

$$\begin{aligned}
 a(t+1) = & a(t)\{a^K(t) + [1 - a^K(t)][p^2 + (1-p)^2]\} + [1 - a(t)] \\
 & \times \{a^K(t)\Phi(p,s;t) + [1 - a^K(t)][\Omega(p,s;t) \\
 & + \Psi(p,s;t)]\}. \tag{5}
 \end{aligned}$$

This equation has a fixed point at the value  $a^* = 1$ ; thus,

$$\left. \frac{\partial a(t+1)}{\partial a(t)} \right|_{a^*=1} = 1 + 2Kp(1-p) - \Phi(p,s) \leq 1 \tag{6}$$

is the condition for the fixed point to be stable, which leads to the following critical surface separating the ordered and disordered phases for annealed RWN's:

$$2Kp(1-p) = \Phi(p,s), \tag{7}$$

where now  $\Phi(p,s) = \Phi(p,s;t \rightarrow \infty)$ , for the stationary distribution  $\{P_n(t \rightarrow \infty)\}_{n=1,\dots,s}$  from Eq. (4).

Notice that when  $s=2$ , then  $\Phi(p,2;t) = 1$  for all  $t$ , which leads to the well-known critical curve for RBN's [9]:

$$K2p(1-p) = 1. \tag{8}$$

#### IV. SIMULATIONS OF ANNEALED AND QUENCHED RWN's

In [8] we showed the evolution of the overlap in RWN's as a function of the number of possible states  $s$  and how the stationary value of the overlap  $a^*$  acts as an order parameter, a RWN being ordered when  $a^* = 1$ . The agreement between annealed simulations and the theoretical overlap evolution model for the annealed case was complete. We also showed how the stationary value of the overlap is smaller as  $s$  grows and how it is always smaller in the annealed model when compared with the quenched model. Nevertheless, none of those simulations were performed near a critical point and its effect was not shown.

In the upper part of Fig. 2 we show the evolution of the overlap  $a(t)$  between two given configurations of an annealed system, given fixed values of  $N$ ,  $K$ , and  $s$ , as a function of the bias  $p$ . Solid lines are the theoretical predictions for annealed RWN's, obtained from Eqs. (4) and (5), and symbols (circles, squares, diamonds, and triangles) mark the results from simulations of annealed RWN's. As  $t$  tends to infinity, these values of  $a(t)$  tend to  $a^*$ , the stationary value of the overlap. Both for the ordered case ( $a^* = 1$ ) with high  $p$  and the disordered case with low values of  $p$ , there is full agreement between our theoretical annealed model and the annealed simulations.

There is only a discrepancy in the special case with  $p = 0.81$ , which corresponds to a critical point. This phenomenon was expected and it is usual in critical points [12]. When the system is at a critical point, the effects of the finiteness of the system are more evident, and the discrepancy is a consequence of the system size. Yet as the systems we simulate become bigger ( $N=100$ ,  $N=1000$ ,  $N=10\,000, \dots$ ), the experimental points tend to converge to the theoretical curve. We should remember the fact that the annealed RWN's are not completely uncorrelated. Even in the annealed case, each automaton still keeps memory of its pre-

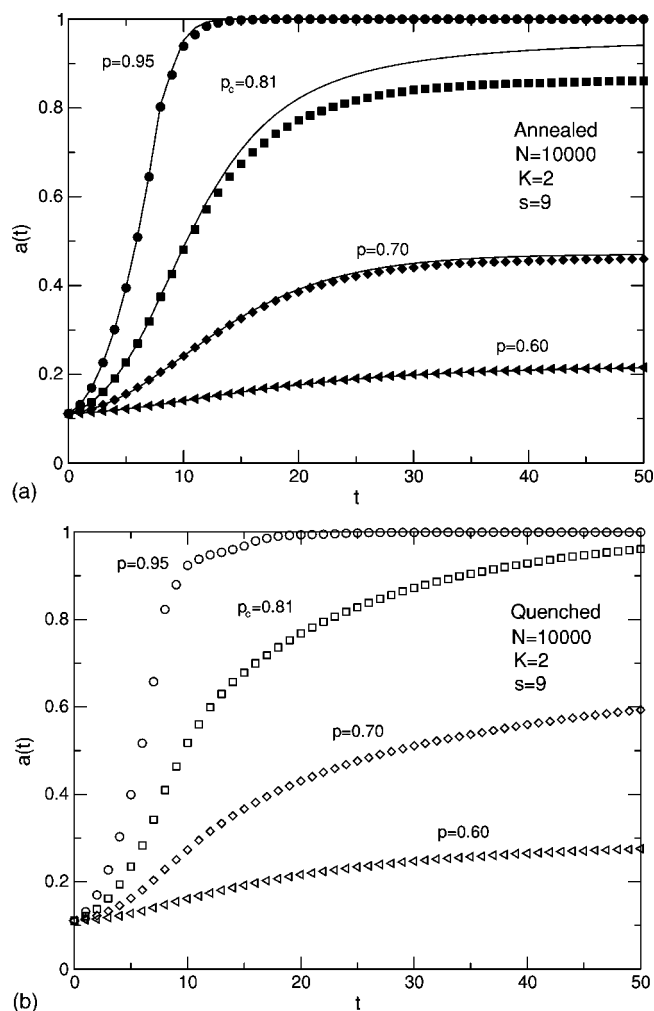


FIG. 2. Evolution of the overlap  $a(t)$  as a function of the bias  $p$ . Top: evolution of the overlap  $a(t)$  for annealed RWN's with  $K=2$ ,  $s=9$ , and different values of the bias  $p$ . In all of them we have taken as initial conditions  $a(0) = 1/s$ . Each point represents the average of 100 different networks, with  $N=10\,000$  automata each one. Solid lines represent the theoretical evolution using Eqs. (4) and (5). Bottom: evolution of the overlap  $a(t)$  for quenched RWN's for the same parameter values and initial conditions than those in the left graph. Again, each point represents the average of 100 different networks, with  $N=10\,000$  automata each one.

vious state, as we mentioned before, and this fact introduces temporal correlations in the annealed model, which are especially evident in the transition points. Nevertheless, the theoretical description of the annealed model is correct at the thermodynamical limit—i.e., when  $N$  tends to infinity. For comparison we also show (Fig. 2, bottom) the quenched model simulations for the same values of the parameters. Clearly, the stationary overlap values for the quenched model are bigger than those for the annealed model. Thus, the latter underestimates the former.

This result implies that the critical values of the bias  $p$  for the order-disorder transition in the annealed model will be larger than in the quenched case. We can see this better in Fig. 3. Here we have calculated the transition points for both quenched and annealed systems, for the case  $K=2$ . These

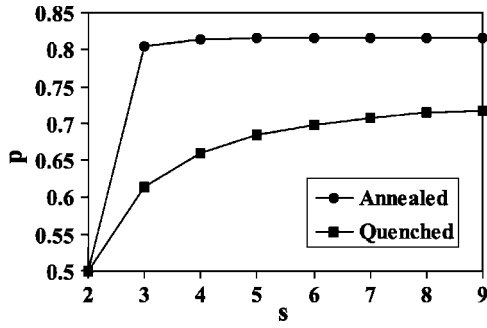


FIG. 3. Order-disorder transition in RWN's. The critical values of the bias for RWN's with  $K=2$  are plotted as a function of the number of states  $s$ , for both annealed and quenched systems. The transition in quenched RWN's happens at values of  $p$  smaller than those predicted by the annealed model.

transition points are defined by the values of  $p$  where  $a^*$  equals 1 for the first time (we can use in fact  $1-a^*$  as the order parameter). It is clear that the annealed model fails to predict the transition for the quenched model. The transition in the quenched model takes place at values of  $p$  smaller than those predicted by the annealed model and hence, in this case, Derrida's method does not work. This failure is an effect of the different state probability distributions  $\{P_n\}_{n=1,\dots,s}$  in both models due to the memory of the quenched system, as we will prove in Sec. V.

Nevertheless, it is important to highlight that in both cases (see Fig. 3) as  $s$  increases the curves quickly converge to a limiting value. This implies that at the continuous limit,  $s \rightarrow \infty$ , the transition is well defined and independent of the value of  $s$  [8].

V. RWN QUENCHED MODEL

In RBN's the frontier between order and disorder obtained using an annealed model coincides with the frontier for the quenched model. As we have seen, this is not the case for RWN's, and the transitions between order and disorder in these two models do not coincide. Such a result is due to the fact that the memory of the quenched system introduces strong correlations in the automata. As a consequence, in the quenched model each automaton is not strictly modified by a pure random-walk perturbation, and the automaton-state distributions in this model are clearly different to the distributions in the annealed method. Observe that the stationary values of  $\{P_n\}_{n=1,\dots,s}$  can be calculated from Eq. (4) in the limit when  $t \rightarrow \infty$  and then summing up all the equations from 1 to a certain  $n$ . In this way we arrive to the following recurrent relationship:

$$P_n = P_{n-1} \left( \frac{p}{1-p} \right). \tag{9}$$

Normalizing to 1 the sum of  $P_n$  from 1 to  $s$ , we obtain

$$P_n = \frac{1}{z} \left( \frac{p}{1-p} \right)^{n-1}, \tag{10}$$

an exponential discrete probability distribution, with the normalization factor equal to

$$z = \frac{1 - \left( \frac{p}{1-p} \right)^s}{1 - \frac{p}{1-p}}. \tag{11}$$

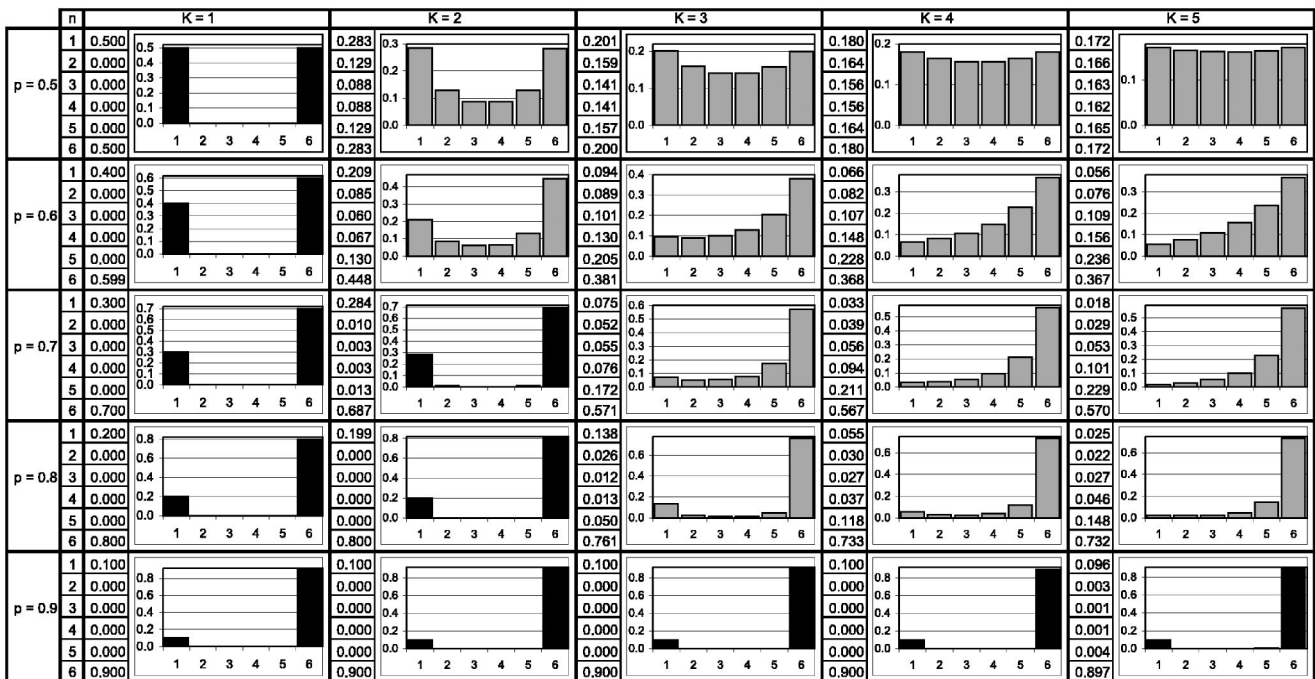


FIG. 4. The stationary automaton-state distribution  $\{P_n\}_{n=1,\dots,6}$  for a quenched RWN in the case  $s=6$  as a function of the bias  $p$  and the connectivity  $K$ . Ordered states are plotted as black bars.

But in fact, the behavior of the automata in the ordered zone is far away from such a biased random walk. The stationary quenched distribution of the automaton values will not be an exponential like the one described by the previous equation.

Figure 4 shows the stationary automaton-state distribution  $\{P_n\}_{n=1,\dots,6}$  for a quenched RWN in the case  $s=6$ . It can be seen that as we enter the disordered zone (i.e., big values of the connectivity  $K$ ) it tends to an exponential distribution, according to Eq. (10). In that zone, each automaton is being perturbed by a nearly pure biased random walk. But in the ordered zone (small values of the connectivity), the distribution tends to be limited basically to the extreme values, 1 or  $s$ , the intermediate states having a probability close to 0. One can see how the ordered state has basically a binary outcome. Notice also that in this zone the probability for an automaton to be  $s$  or 1 is clearly determined by the bias  $p$ , being  $p$  and  $(1-p)$ , respectively.

If we now use the stationary quenched values of the automata distribution in the ordered zone—that is, if we use

$$P_n = \begin{cases} (1-p) & \text{if } n = 1, \\ p & \text{if } n = s, \\ 0 & \text{otherwise,} \end{cases} \quad (12)$$

and we apply them to Eq. (7), we obtain that the boundary condition becomes

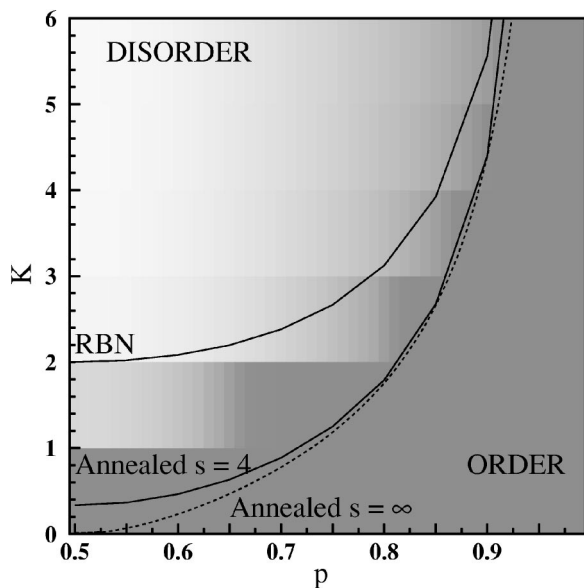


FIG. 5. Gray pixels: stationary overlap  $a^*$  between two quenched RWN's as a function of  $p$  and  $K$ . Gray intensities indicate different values of the stationary overlap. Dark gray corresponds to a perfect overlap—that is, to  $a^* = 1$  (ordered phase)—and white to noncorrelated  $a^*$  (completely disordered phase). For each point we have performed 10 000 simulations with  $N=10\,000$  and  $s=4$ . Superimposed are the order-disorder frontiers for RBN's (upper solid line) and for the annealed model of RWN's (lower solid line) in the case  $s=4$ . We can see how the transition from order to disorder in the quenched RWN's happens in the zone between both curves. The dashed line corresponds to the critical  $K$ - $p$  curve from Eq. (12) in the annealed case when  $s \rightarrow \infty$ .

$$K2p(1-p) = 1, \quad (13)$$

that is, again, the boundary condition for RBN's.

Therefore, RBN's and the annealed model of RWN's are the limiting cases for quenched RWN's (coinciding only in the case  $s=2$ ), and the critical transition order-disorder curve for quenched systems lies between both transition frontier curves, as can be seen in Fig. 5.

As Fig. 3 implies, when passing from these discrete networks to the continuous case—that is, when  $s$  tends to infinity—the transition from order to disorder is still well defined. It is possible to calculate the limit of Eq. (7) for annealed RWN's when  $s \rightarrow \infty$ . In the continuous case, the critical curve becomes

$$K = \frac{2[p - (1-p)]^2}{p(1-p)[1 + |p - (1-p)|]^2}, \quad (14)$$

which defines an order-disorder critical curve in the  $K$ - $p$  space (Fig. 5, dashed line). Equation (13) can be expressed in a more compact form, but we prefer to write it this way because it explicitly shows its invariance under the exchanges of  $p$  and  $(1-p)$ .

As the annealed model is a lower limit (in the  $K$  axis; upper in the  $p$  axis) of the quenched systems, then for quenched RWN's in the continuous limit ( $s \rightarrow \infty$ ) the transition is also well defined and enclosed between the annealed model and the classical transition for RBN's.

## VI. CONCLUSIONS

The study of the genome has revealed a complex world of relationships and couplings among genes, which produces what is indeed a genetic network. As a consequence, the study of its behavior by means of classical, linear methods is not possible given that the real behavior is highly nonlinear and shows complex dynamics. Therefore new type of models and methods of analysis are needed to face its study and understanding.

RBN's were one of the first ways proposed to study statistically genome global properties. Unfortunately this is a model of all-nothing behavior where the state of a given gene is completely determined by the input genes and where smooth variations of state are not allowed, contrary to what happens in the real genomes. On the other hand, differential equation systems, which in principle should give a better understanding of such continuous behavior, are difficult to solve and analytical results are hard to obtain.

This paper deals with random walk networks, a simple random network model which largely resembles real genetic networks. RWN's are a natural link between discrete all-nothing models (like RBN's) and continuous differential equations systems, as RWN's allow small, continuouslike variations in the behavior of the genome.

RWN's allow for analytical treatment, and in this paper we have deduced the critical frontier for the annealed model. Unfortunately, due to the memory of the system, the annealed solution does not coincide with the quenched critical frontier. Nevertheless, the annealed critical boundary acts as a lower limit for the real case. On the other hand, we have

shown how RBN's act as an upper limit for the quenched case and we have delimited its order-disorder transition frontier to be between both transition frontiers. If RWN's pretend to be a bridge model between RBN's and continuous models, we have demonstrated that in the continuous limit ( $s$  tending to infinity) RWN's are well behaved and, as RBN's, have a well-defined order-disorder transition, usually so difficult to prove for continuous systems.

As we have seen, RWN's can be considered a natural generalization of RBN's. In fact, RBN's are a subcase of our model which trivially reduce to them when the number of allowed states  $s$  equals 2. RBN's have been studied extensively over the past three decades [13] and are still used as a

model to study competitive games [14], synchronization [15,16], scale-free connectivity [17,18], self-organized criticality [19], or time-reversible models [20,21]. RWN's now offer a more general and richer frame to study all these phenomena.

#### ACKNOWLEDGMENTS

We would like to thank Amelia Ortiz and Alberto Fernández for their valuable opinions. B.L. has been supported by CICYT BFM2002-01812. F.B. has been supported by MEC AYA 2003-08739-c02-0 (including FEDER) and Generalitat Valenciana GRUPOS 03/170.

- 
- [1] S. Bornholdt, *Biol. Chem.* **382**, 1289 (2001).  
 [2] S. A. Kauffman, *J. Theor. Biol.* **22**, 437 (1969).  
 [3] S. A. Kauffman, *The Origins of Order* (Oxford University Press, New York, 1993).  
 [4] D. Kaplan and L. Glass, *Understanding Nonlinear Dynamics* (Springer-Verlag, New York, 1995).  
 [5] T. A. Brown, *Genomes* (Wiley, New York, 1999).  
 [6] R. Thomas, D. Thieffry, and M. Kaufman, *Bull. Math. Biol.* **57**, 247 (1995).  
 [7] K. Kappler, R. Edwards, and L. Glass, *Signal Process.* **83**, 789 (2003).  
 [8] B. Luque and F. Ballesteros, *Physica A* **342**, 207 (2004).  
 [9] B. Luque and R. V. Solé, *Phys. Rev. E* **55**, 257 (1997).  
 [10] T. Rohlf and S. Bornholdt, *Physica A* **310**, 245 (2002).  
 [11] J. A. de Sales, M. L. Martins, and D. A. Stariolo, *Phys. Rev. E* **55**, 3262 (1997).  
 [12] B. Derrida and Y. Pomeau, *Europhys. Lett.* **1**, 45 (1986).  
 [13] M. Aldana, S. Coppersmith, and L. P. Kadanoff, in *Perspectives and Problems in Nonlinear Science*, Springer Applied Mathematical Sciences Series, edited by E. Kaplan, J. E. Marsden, and K. R. Sreenivasan (Springer-Verlag, Berlin, 2003).  
 [14] I. Nakamura, *Phys. Rev. E* **65**, 046128 (2002).  
 [15] L. G. Morelli and D. Zanette, *Phys. Rev. E* **63**, 036204 (2001).  
 [16] F. J. Ballesteros and B. Luque, *Physica A* **313**, 289 (2002).  
 [17] J. J. Fox and C. C. Hill, *Chaos* **11**, 809 (2001).  
 [18] C. Oosawa and M. A. Savageau, *Physica D* **170**, 143 (2002).  
 [19] B. Luque, F. J. Ballesteros, and E. M. Muro, *Phys. Rev. E* **63**, 051913 (2001).  
 [20] S. N. Coppersmith, L. P. Kadanoff, and Z. Zhang, *Physica D* **149**, 11 (2001).  
 [21] S. N. Coppersmith, L. P. Kadanoff, and Z. Zhang, *Physica D* **157**, 54 (2001).